Supersonic Propeller Noise in a Uniform Flow

Wen-Huei Jou*
Flow Research Company, Kent, Washington

The sound field produced by a supersonic propeller operating in a uniform flow is investigated. The main interest is the effect of the finite forward flight speed on the directivity of the sound field as seen by an observer on the aircraft. The integral representation of the solution to the convective wave equation is obtained by using Green's function. The source space is transformed to a blade-fixed coordinate for ease of evaluation. The solution in frequency domain is obtained through Fourier transformation of the solution in the time domain. By using a far-field approximation, the solution is simplified to a form from which qualitative directivity pattern can be extracted. It is found that there are cones of silence on the axis of the propeller. The semiapex angles on these cones are equal fore and aft of the propeller plane and depend on the tip Mach number only. The Fourier coefficients of the acoustic pressure contain the Doppler amplification factor $[(1 - M^2 \sin^2\Omega)^{1/2} - M \cos\Omega]^{-1}$. The sound field weakens in the upstream direction and strengthen downstream. Kinematic considerations of the emitted Mach waves not only confirm these results, but also provide physical insight into the sound generation mechanism. The predicted zone of silence and the Doppler amplification factor are compared to the theoretical prediction of shock wave formation and the flight test of the SR3 propeller.

Introduction

THE early work of Gutin[1] on the noise generated by an open rotor is known to be applicable only to the subsonic propellers. At high speeds, the acoustic wave length becomes comparable with the length scale of the blade. The source can not be considered "compact" as implied by Gutin's theory.

The general theory of sound generated by a surface in arbitrary motion was investigated by Ffowcs Williams and Hawkings.[2] The acoustic sources due to the motion of a solid surface were identified as the volume displacement, surface force, and flowfield effects. Each of these behaves as an acoustic monopole, dipole, and quadrupole, respectively. The general solution is then constructed in integral form by using the fundamental solution of the wave equation. The Dirac delta function in the integrand projects the integral into a three-dimensional subspace. This subspace can be chosen at will by using various basis vectors for analytical or computational convenience. Thus, the solution can be presented in various forms.

One of the most important forms of the general solution is that obtained by projection to the three spatial dimensions. The procedure results in the familiar retarded potential solution. With further transformation of the spatial domain from the inertial frame to a coordinate system fixed on the solid surface, the integrand for integration in space domain can be shown to be singular when the relative velocity of the surface to the observer is at sonic speed. One may also project the four-dimensional integral to the surface of a sphere collapsing at sonic speed toward the observer. This form of the solution avoids the above-mentioned singularity, but creates a new singularity when the solid surface is moving toward the field point at sonic speed with its normal in the direction of radiation.

The general theory of Ffowcs Williams and Hawkings has been applied to the supersonic rotor noise in various forms. Hawkings and Lowson[3] employed the retarded potential approach in a blade-fixed coordinates. They solved the problem in the frequency space and constructed the time wave form by Fourier inversion. The singularity in the integrand was shown to be integrable and the Fourier coefficients were obtained by using a far-field approximation. They found that there are cone of silences fore and aft of the propeller plane, in which the supersonic noise is exponentially small. Whitham's[4] theory of weak shock propagation was then applied to examine the nonlinear distortion of the time waveform as it propagated into the far field. Hawkings and Lowson showed that the nonlinear effects substantially alter the waveform, but have little effect on the overall sound pressure level. Finally, they concluded that the linear theory can be used as a predictive tool for the gross features of the acoustic field.

On the other hand, Farasset and Brown[5] employed the approach using the collapsing-sphere solution of Ffowcs Williams-Hawkings's general theory. To obtain the time waveform of the acoustic signature, a collapsing sphere, centered at the observer, is generated from infinity at each observer's time. As the sphere collapses toward the observer at sonic speed, the intersection of the sphere and the rotating blade surface can be computed. This intersection generates a surface and the acoustic signal at the observer's time can be computed by integrating the contributions from the sources over that surface. The method may be implemented by using a mean surface approximation or by using the exact location of the solid surface. The numerical computations were later made very efficient.[6] The procedure is entirely numerical and no far-field approximation is made. The noise field can be mapped out by calculating the signature at different observer's positions.

Although Farassat and Brown's procedure, aside from the discretization error, is an exact solution of the linear acoustic equation and, hence, more accurate than that by Hawkings and Lowson[3] in the near field, the latter explicitly showed some very interesting characteristics of the sound field of a supersonic rotor. The existence of the silent zone in front of and behind the rotor is particularly useful information. Other characteristics and physical insights can also be obtained by using the approach of Hawkings and Lowson.[3]

The aerodynamic field as observed on a blade-fixed coordinate system is in steady state. If such a steady-state solution can be found, the azimuthal variation of the pressure field away from the propeller can be easily transformed to time domain as acoustic waveform. Jou[7] numerically solved the exact nonlinear potential flow in a blade-fixed, body-fitted three-dimensional grid system. However, the attention was

Received Aug. 21, 1987; revision received April 4, 1988.

*Vice President and Senior Research Scientist.

mainly given to the near-field flow structure. The computational grid was clustered near the propeller surfaces with very few grid points in the far field. Therefore, prediction of the acoustic waveform was not attempted. On the other hand, Tam and Salikuddin[8] assumed that the near field is governed by linear potential flow and that the cumulative nonlinear effect along the path of propagation results in the formation of shock waves. Therefore, they formulated a linear aerodynamic near-field problem with nonlinear effects restored in the far field. The predicted waveforms at various location were compared favorably to those obtained from the flight tests.

Hanson[9,10] examined the far- and near-field noise in frequency domain. The theory incorporated the effects of the forward flight by considering the helically convected steady source distribution. The effect of the blade sweep on the noise was shown to result in phase cancellation of the signals generated at different spanwise sections. The time waveform was obtained by Fourier synthesis and was, in general, in good agreement with experimental measurements.

The various predictive methods developed in recent years provide valuable tools for design purposes. The present paper complements these methods by attempting to extract qualitative physics from an extension of Lowson and Hawkings theory. The major extension is the inclusion of the effects of the finite forward flight speed. This modification is essential for examination of the cabin noise. By using a far-field approximation, some information on the directivity pattern can be directly extracted. Particularly, we address the question of whether the cones of silence will maintain the symmetry with respect to the rotor plane and of how the forward flight speed will modify the directivity pattern through Doppler amplification effects. These simple results are compared with the theoretical prediction of Tam and Salikuddin[8] and the flight test of the SR3 propeller.

Retarded Potential Solution for Convective Wave Equation

The starting point of the following analysis is that the wave front propagates in a uniform flow as a convective sphere.[4] Based on this idea, it is fairly easy to construct the fundamental solution of the convective wave equation and to obtain the general solution in an integral form.

Consider an acoustic disturbance generated at A and propagating in a medium with a speed of sound a and a convective Mach number M. The signal propagates away from A as a convected sphere, as shown in Fig. 1.

Referring to Fig. 1, the center of the convected spherical wave front is at B. For an observer at C, the received strength of the signal is inversely proportional to $\hat{r}$. By simple geometrical construction, the following relation between the distance r, from the observer to the emitter, and $\hat{r}$ can be obtained:

$$(\hat{r}/r) = (K^2 + \beta^2)^{1/2} - K \tag{1}$$

where

$$K = (M \cdot e_r)\beta^2 \tag{2}$$

$$\beta = (1 - M^2)^{-1} \tag{3}$$

where e_r is the unit vector pointing from A toward C. The retarded time to the observer at C is simply

$$\tau_0 = t - (\hat{r}/a) \tag{4}$$

Using Eqs. (1-4), the solution to the convective wave equation with a nth-pole source $Q_{ij\ldots}$, can be given as

$$4\pi(p - p_0) = \frac{\partial^n}{\partial x_i \partial x_j \ldots} \cdot \int Q_{ij\ldots}(y,\tau)\, \frac{\delta(\tau - \tau_0)}{\hat{r}}\, dy\, d\tau \tag{5}$$

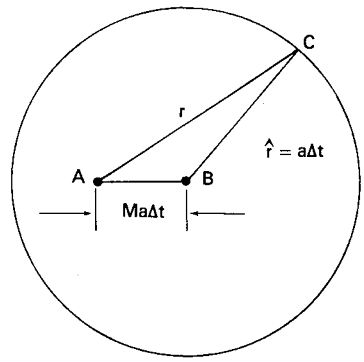

Fig. 1 Wave front geometry.

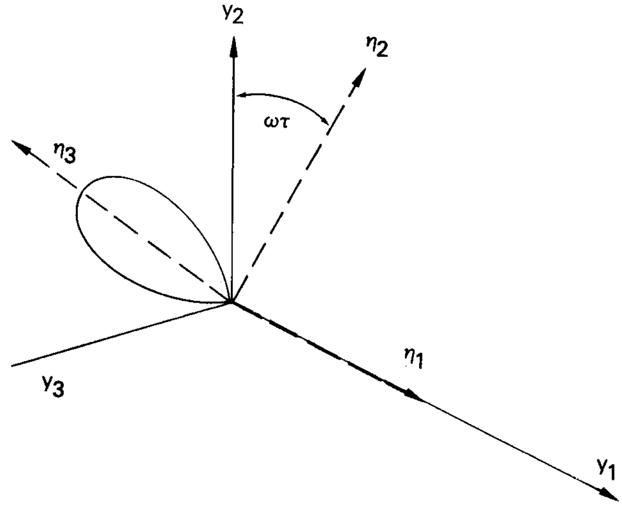

Fig. 2 Blade-fixed coordinate.

where $(p - p_0)$ is the acoustic pressure. In the solution given by Eq. (5), the source space y is in a coordinate system fixed in a nonrotating frame. The moving body (emitter) is regarded as distributed pulsating sources whose strength is nonzero only when the solid surface passes through the field point y.

For describing acoustic disturbances generated by a rotating propeller, the most appropriate coordinate system for describing the sources is that of a blade-fixed coordinate as shown in Fig. 2. The source strength described in such a system is in a steady state. The acoustic signal at the observer's position x and at the observer's time can then be obtained by summing the contributions from the steady sources emitted at the position related to the observer's space-time (x,t) by the retarded time.

The transformation from the inertial frame y to the blade-fixed coordinate η is defined by

$$y_1 = \eta_1 \tag{6}$$

$$y_2 = \eta_3 \sin\omega\tau + \eta_2 \cos\omega\tau \tag{7}$$

$$y_3 = \eta_3 \cos\omega\tau + \eta_2 \sin\omega\tau \tag{8}$$

$$\tau = t - (r/a)[(K^2 + \beta^2)^{1/2} - K] \tag{9}$$

Without loss of generality, we assume that the initial phase of rotation is zero. Since r and e_r depend on the variable y, the above transformation is implicit. The Jacobian of the transformation can be shown to be

$$J = \det\left(\frac{\partial y_i}{\partial \eta_j}\right) = \left(1 + U_i \frac{\partial \tau}{\partial y_i}\right)^{-1} \tag{10}$$

where U_i is the velocity of the emitter. Note that for $M = 0$, so that $K = 0$ and $\beta = 1$, Eq. (10) reduces to the corresponding expression given by Ffowcs Williams and Hawkings[2] and Lowson[11]; i.e.,

$$J = [1 - (U/a) \cdot e_r]^{-1} \tag{11}$$

With these transformations, the general solution [Eq. (5)], can be rewritten in the following form:

$$4\pi(p - p_0) = -\frac{\partial}{\partial x_j} \int \left[\frac{f_j}{\hat{r}} J \right] \mathrm{d}S - \frac{\partial}{\partial t} \int \left[\frac{\rho_0 a (m + M) \cdot \nabla h}{\hat{r}} J \right] \mathrm{d}S \tag{12}$$

where the brackets [ ] denote the values of the quantities at the retarded time, h the thickness of the blade, m the rotation Mach number of the emitting element, and the integrations are evaluated over the planform of the blade. Here, a thin blade is assumed. Therefore, the forces on the top and the bottom surfaces of the blade are combined to give the net force f_j on the planform of the blade.

Fourier Components of Acoustic Pressure

We now expand the acoustic pressure given by Eq. (12) in Fourier series in time. Since the integrands are described in the space-time domain on a blade-fixed coordinates, the Fourier integral in the observer's time domain may be transformed to that in the emitter's time domain. The difference between the observer's time t and the emitter's time τ is the time of flight of the acoustic signal Δt as shown in Fig. 1. Therefore,

$$\tau + \Delta t[y(\tau)] = t \tag{13}$$

Since,

$$\frac{\mathrm{d}y_i}{\mathrm{d}\tau} = U_i \tag{14}$$

and

$$\frac{\partial(\Delta t)}{\partial y_i} = \frac{\partial \tau}{\partial y_i} \tag{15}$$

the transformation from the observer's time to the emitter's time can be shown to be

$$\mathrm{d}t = J^{-1}\, \mathrm{d}\tau \tag{16}$$

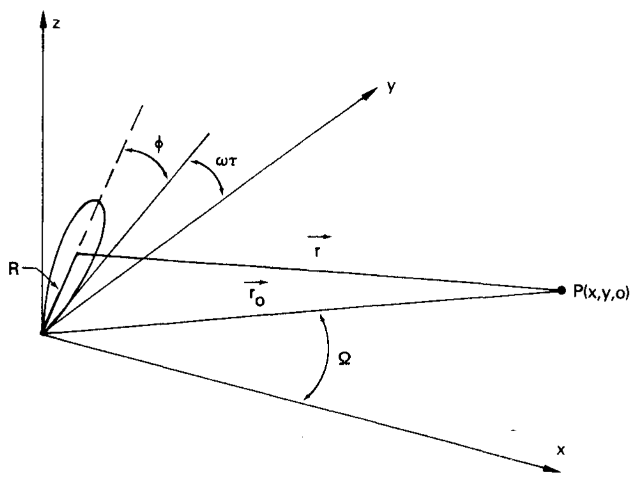

Fig. 3 Polar coordinates.

This transformation leads to the following expression for the Fourier coefficients for the acoustic pressure:

$$C_n = \frac{1}{4\pi} \int \left(in\omega I - \frac{\partial}{\partial x_j} I_j \right) \mathrm{d}S \tag{17}$$

where ω is the frequency of the rotation, n the harmonic number, and

$$I = \frac{\omega}{\pi} \int_0^{2\pi/\omega} \frac{\rho_0 a (m + M) \cdot \nabla h}{\hat{r}} \cdot \exp\left[in\omega \left(\tau + \frac{\hat{r}}{a} \right) \right] \mathrm{d}\tau \tag{18}$$

and

$$I_j = \frac{\omega}{\pi} \int_0^{2\pi/\omega} \frac{f_j}{\hat{r}} \cdot \exp\left[in\omega \left(\tau + \frac{\hat{r}}{a} \right) \right] \mathrm{d}\tau \tag{19}$$

For a propeller with supersonic tip speed, the wave length $a/n\omega$ is comparable to the length of the blade R, because $\omega R/a = O(1)$. The source is noncompact and cannot be considered as a concentrated source even in the far field.

In order to simplify the expression for C_n and to extract physical information on the mechanism for sound generation, we consider the far field approximation as the limit that $R/r \ll 1$ and $a/n\omega r \ll 1$. In the far field, the observer's position is defined in a spherical polar coordinate system (r_0, Ω, 0) as shown in Fig. 3. Since the sound field is axisymmetric, the azimuthal angle is set to be zero. To the first order of far-field approximation, we have

$$\hat{r} \approx \frac{r_0}{1 - M^2} \left[(1 - M^2 \sin^2\Omega)^{1/2} - M \cos\Omega - \frac{1 - M^2}{(1 - M^2 \sin^2\Omega)^{1/2}} \sin\Omega \cos\theta \frac{R}{r_0} \right] \tag{20}$$

where

$$\theta = \omega\tau + \phi \tag{21}$$

and the meridian angle for the observer's position is defined by

$$\sin\Omega = y/r_0 \tag{22}$$

Letting $m = \omega R/a$ be the rotation Mach number of the emitting element, the integral in Eq. (18) can be evaluated to give

$$I = \frac{2\rho_0 a (m + M) \cdot \nabla h (1 - M^2)}{r_0 K_D} J \Bigg] \times \exp\left[\frac{in\omega r_0}{a(1 - M^2)} K_D - in\phi - \frac{in\pi}{2} \right] J_n(nY) \tag{23}$$

where J_n is the Bessel function in which the argument Y is

$$Y = \frac{m \sin\Omega}{(1 - M^2 \sin^2\Omega)^{1/2}} \tag{24}$$

and the Doppler amplification factor K_D is defined as

$$K_D = (1 - M^2 \sin^2\Omega)^{1/2} - M \cos\Omega \tag{25}$$

The force on the blade f_j is decomposed into the thrust component T and the drag component D, which is in the tangential direction of the circular path of the rotation, as

$$f_j = (-T, -D \sin\theta, D \cos\theta) \tag{26}$$

With quite a bit of algebra,[9] the second term of the integrand in Eq. (17), which is the contribution from the force on the blade, can be represented by the sum of the following two expressions:

$$\left[\frac{\partial l_j}{\partial x_j}\right]_T = -\frac{2in\omega}{ar_0K_D}\exp\left[\frac{in\omega r_0K_D}{a(1-M^2)} - in\phi - \frac{in\pi}{2}\right] \times J_n(nY)\cdot\left[\frac{\cos\Omega}{(1-M^2\sin^2\Omega)^{1/2}} - M\right]T \tag{27}$$

$$\left[\frac{\partial l_j}{\partial x_j}\right]_D = \frac{2in\omega}{aK_Dr_0}\frac{1-M^2}{m}J_n(nY)D \times \exp\left[\frac{in\omega K_Dr_0}{a(1-M^2)} - in\phi - \frac{in\pi}{2}\right] \tag{28}$$

In these expressions, we have taken only the leading terms in the expansions under the far-field approximation. By substituting Eqs. (18), (27), and (28) into Eq. (17), we finally arrive at an expression for the Fourier coefficient C_n as

$$C_n = \frac{in\omega}{2\pi aK_Dr_0}\exp\left[\frac{in\omega r_0K_D}{a(1-M^2)} - \frac{in\pi}{2}\right] \times \iint\left[\rho_0a^2(m+M)\cdot\nabla h(1-M^2)\right] \times\left\{+T\left[\frac{\cos\Omega}{(1-M^2\sin^2\Omega)^{1/2}} - M\right] - \frac{D(1-M^2)}{m}\right\} \times J_n(nY)\exp(-in\phi)(\cos\sigma)^{-1}Rd\,Rd\phi \tag{29}$$

where the rotational Mach number m, distributed force (T,D), and thickness distribution h are functions of the coordinates (ϕ,R) on the blade surface and σ is the twist angle of the blade.

We have achieved in Eq. (29) in reducing the expression for the Fourier coefficient of the acoustic pressure at an observer's location x to a surface integral on the blade planform surface.

One interesting and perhaps useful feature of Eq. (29) can be observed. For a fixed radius R, the ϕ integral is the Fourier integral of the blade thickness h and the force (T,D). With proper arrangement of the planform shape, the R integral may give a favorable phase cancellation effects for those particular harmonics.

Zone of Relative Silence and Doppler Amplification

Some important characteristics, particularly the directivity pattern, of the acoustic disturbances can be extracted from Eq. (29).

The Bessel function $J_n(nY)$ is exponentially small for $Y<1$. This is particularly true for high harmonics, i.e., large n. Therefore, $Y<1$ defines a zone of relative silence where only the subsonic Gutin's noise exists. From the definition of the variable Y [Eq. (24)], we can derive the following bound on the meridian angle Ω for the zone of silence:

$$\pi - \sin^{-1}\frac{1}{M_{\text{tip}}} \le \Omega \le \sin^{-1}\frac{1}{M_{\text{tip}}} \tag{30}$$

where M_{tip} is the tip Mach number which is the vector sum of the forward flight velocity and the rotational velocity at the tip.

This result shows that the zone of relative silence is a pair of cones with the flight direction as its axis. The semiapex angles of the cones of silence fore and aft of the rotor plane remain symmetric even in the cases with forward flight velocity. (See Fig. 4.) The angle is entirely dependent on the tip Mach number and is independent of the individual components of the forward flight and rotating Mach numbers. In the first sight, this result is surprising. However, Hayes[12] confirmed this result by considering the ray path of the emitted Mach

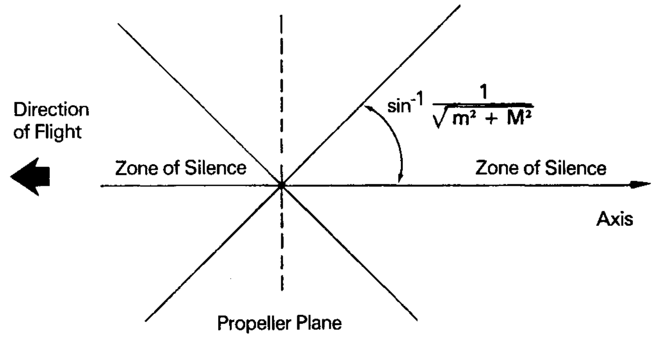

Fig. 4 Zone of silence.

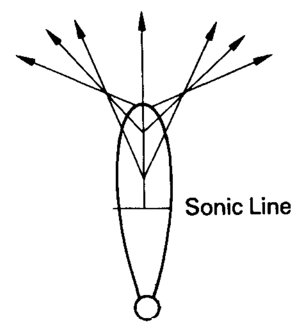

Fig. 5 Rays of Mach waves.

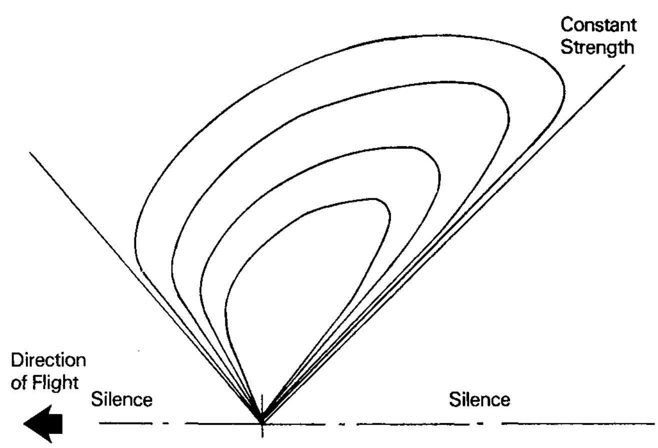

Fig. 6 Qualitative directivity.

waves. He computed the envelope of the ray cones generated by a rotating source in a uniform flow and found that the envelopes are cones with the semiapex angle given by Eq. (30). Referring to Fig. 5, one can see immediately that the Mach waves propagate sideway into a region confined by the envelopes of the ray cones emitted at the tip of the propeller.

Tam and Salikuddin[8] computed the radial distance of the shock formation along the direction of propagation as a function of the meridian angle Ω for a SR3 propeller operating at a flight Mach number of 0.8. The tip rotational Mach number was 0.825. They showed that for $65<\Omega<120$ deg, shock waves are formed, but that there is no shock formation outside of this range because of the weak sound level. Using the operating condition, the tip Mach number M_{tip} is 1.15. The corresponding Ω range of strong acoustic disturbance can be

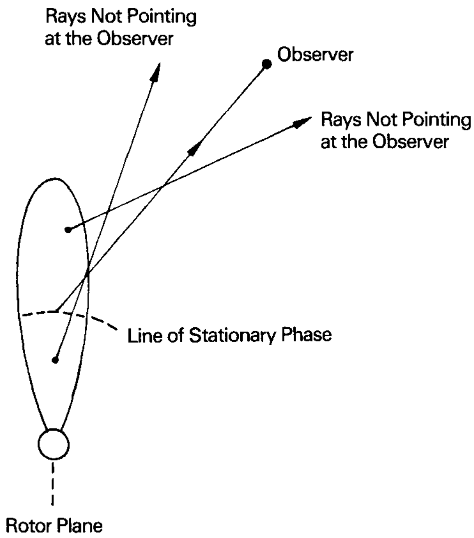

Fig. 7 Radius of stationary phase and ray.

computed by using Eq. (30) and is $60<\Omega<120$ deg. This is in very good agreement with the results by Tam and Salikuddin.[8]

It can also be observed that the strength of the acoustic disturbances decays as $(K_D r_0)^{-1}$, where K_D is the Doppler amplification factor. K_D is defined by Eq. (25) and is dependent on the meridian angle Ω. Therefore, the strength of the signal is stronger in the downstream direction and is weakened in the upstream direction, as one would expect intuitively. Figure 6 shows the qualitative directivity pattern as discussed in the last paragraph. A similar picture indicating the wave front geometry was given be Lowson and Jupe[13] based on a kinematic consideration of the wave front propagation.

Limited information on the directivity pattern obtained from the flight test of the SR3 propeller together with the computed results were given by Tam and Salikuddin.[8] Figures 13 and 14 of their paper presented the wave forms at $\Omega = 110$ and 73 deg, respectively. To examine the directivity pattern, the peak value of the pressure wave form is chosen as the strength of the signal. If one computes the ratio between the peak of the pressure waveform at $\Omega = 73$ deg and that at $\Omega = 110$ deg, the experimental value is approximately 2.2. The ratio of the signal strength at these two locations can also be estimated by using the Doppler's factor and is approximately 2.27. Although the detailed waveform at various locations depends on the distribution of the sources on the blade surface, the agreement between the predicted and experimental values as discussed above is probably more than coincidental. In the present theory, the Doppler's amplification factor is applied to all frequency components. Therefore, an integrated norm of the time waveform is probably a better quantity for verification of the predicted directivity pattern. Nevertheless, the comparison given above seems to support the qualitative directivity pattern obtained by the present theory.

Asymptotic Evaluation of Noise Field for High Harmonics

For supersonic acoustic disturbances, we are expecting a spectrum rich in high harmonics. An asymptotic evaluation of the integral in Eq. (29) in the limit of large n can further simplify the expression and give further insight into the nature of the acoustic disturbances. Following Hawkings and Lowson[3] again, we use the method of stationary phase to evaluate the integral in Eq. (29).

The phase function under consideration is

$$\psi = \omega\left(\tau + \frac{\hat{r}}{a}\right) = \theta + \frac{\omega\hat{r}}{a} \tag{31}$$

where $\hat{r}$ is a function of the polar coordinate (R, θ) and is given by Eq. (20). The stationary point can be easily obtained as

$$\theta_0 = \frac{3\pi}{2}, \qquad \frac{\omega R_0}{a} = \frac{(1-M^2\sin^2\Omega)^{1/2}}{\sin\Omega} \tag{32}$$

Since $\omega R/a = m$, Eq. (32) indicates that the main contribution to the acoustic signal comes from a blade section where the ray is directly pointing toward the observer, as shown in Fig. 7.

The approximate Fourier coefficients for high frequency are then given by

$$C_n = \frac{i}{2\pi}\frac{(1-M^2\sin^2\Omega)^{1/2}}{\sin\Omega}\frac{(1-M^2)}{K_D r_0}\cdot\exp\left[-\frac{in\pi}{2}+\frac{in\omega r_0 K_D}{a(1-M^2)}\right]$$
$$\times\int\left\{\left[\rho_0 a^2(m+M)\cdot\nabla h+\frac{T}{(1-M^2)}\right.\right.$$
$$\times\left(\frac{\cos\Omega}{(1-M^2\sin^2\Omega)^{1/2}}-M\right)$$
$$\left.\left.-\frac{D\sin\Omega}{(1-M^2\sin^2\Omega)^{1/2}}\right]\frac{R}{\cos\sigma}\right\}_{R=R_0} e^{-in\phi}\,d\phi \tag{33}$$

The asymptotic evaluation of the Fourier integral reduces the surface integral to a line integral along the chord of a blade section where the emitted ray directly points at the observer. In Eq. (33), one can observe that the high-frequency components of the thickness noise is essentially the Fourier coefficients of the slope of the blade surface. For a blade leading edge with a finite slope, e.g., diamond airfoil, the slope has a finite discontinuity there. It can be easily verified that the Fourier coefficients of a function with finite discontinuity behaves as n^{-1} for large n. For an airfoil with a blunt leading edge, the slope is singular as $\phi^{-1/2}$. The Fourier coefficient decays slowly as $n^{-1/2}$ for large n. This is the radiating singularity as was discussed by Tam.[14] These singularities are integrable. Hence, an integrated norm of the noise such as the over all sound pressure level can still be defined and well predicted by the linear theory.[3]

Conclusions

The present analysis extends the work of Hawkings and Lowson[3] to include a finite forward flight speed. The solution to the convective wave equation is constructed by using the fundamental solution. The intent of the analysis is to provide some physical insights into the characteristics of the sound field, particularly the effects of the forward flight speed to the directivity pattern. These information are important for studying the "cabin" noise when observers are traveling with the aircraft. It is found that the cones of silence exist fore and aft the propeller plane. The semiapex angle of these cones is shown to be $\Omega = \sin^{-1} 1/M_{\text{tip}}$, which is symmetric with respect to the propeller plane. This symmetric characteristics of the cones of silence was explained by the ray path of the emitted Mach waves. The Doppler amplification factor strengthens the signal downstream, while weakening the upstream one. These information are extremely useful in planning the position of the propeller with respect to the cabin to minimize noise and acoustic treatment.

Acknowledgments

The present work was supported by NASA Ames Research Center under Contract NAS2-9807. The author would like to thank Prof. Wallace D. Hayes of Princeton University for several stimulating discussions. The original work was completed in 1979 and was presented at the 17th Aerospace Science Conference as AIAA Paper 79-0348. Since then, the author has left the research subject. He would like to express his gratitude to the two reviewers of the original draft for bringing his attention to several recently published research results that enabled him to revise the paper to its present form.

References

[1]Goldstein, M. E., *Aeroacoustics,* National Technical Information Services, NTIS N74-35118, pp. 230–244, 1974.

[2]Ffowcs Williams, J. E. and Hawkings, D. L., "Sound Generated by Turbulence and Surface in Arbitrary Motion," *Proceedings of the Royal Society of London,* Ser. A., Vol. 264, 1969, pp. 321–342.

[3]Hawkings, D. L. and Lowson, M. V., "Theory of Open Supersonic Rotor Noise," *Journal of Sound and Vibration,* Vol. 36, No. 1, 1974, pp. 1–20.

[4]Whitham, G. B., *Linear and Non-Linear Waves,* Wiley, New York, 1974.

[5]Farassat, F. and Brown, T. J., "A New Capability for Predicting Helicopter Rotor and Propeller Noise Including the Effect of Forward Motion," NASA TM X-74037, 1977.

[6]Farassat, F., "Prediction of Advanced Propeller Noise in the Time Domain," *AIAA Journal,* Vol. 24, April 1986, pp. 578–584.

[7]Jou, Wen-Huei, "Finite Volume Calculation of Three-Dimensional Potential Flow Around a Propeller," *AIAA Journal,* Vol. 21, Oct. 1983, pp. 1360–1364.

[8]Tam, C. K. W. and Salikuddin, M., "Weakly Nonlinear Acoustic and Shockwave Theory of the Noise of Advanced High-Speed Turbopropellers," *Journal of Fluid Mechanics,* Vol. 164, 1986, pp. 127–154.

[9]Hanson, D. B., "Compressible Helicoidal Surface Theory for Propeller Aerodynamics and Noise," *AIAA Journal,* Vol. 21, 1983, p. 881.

[10]Hanson, D. B., "Near Field Frequency-Domain Theory for Propeller Noise," *AIAA Journal,* Vol. 23, April 1984, pp. 499–504.

[11]Lowson, M. V., "The Sonic Field of Singularities in Motion," *Proceedings of the Royal Society of London,* Ser. A, Vol. 286, 1965, pp. 559–572.

[12]Hayes, W. D., Private communication, 1978.

[13]Lowson, M. V. and Jupe, R. J., "Wave Forms for a Supersonic Rotor," *Journal of Sound and Vibration,* Vol. 37, No. 4, 1974, pp. 475–489.

[14]Tam, C. K. W., "On Linear Acoustic Solutions of High Speed Helicoptor Impulsive Noise Problems," *Journal of Sound and Vibration,* Vol. 89, 1983, pp. 119–134.